JOURNAL OF APPLIED POLYMER SCIENCE VOL. 21, 2319–2340 (1977)

Environmental Stress Cracking of Polyethylene

C. J. SINGLETON, E. ROCHE, and P. H. GEIL, *Department of Macromolecular Science, Case Western Reserve University, Cleveland, Ohio 44106*

Synopsis

Deformation of polyethylene in environmental stress cracking (ESC) agents results in changes in both the mechanism of deformation and structure of the resulting drawn material. Stress-cracked failure surfaces are highly fibrillar, the fibrils having less elastic recovery than those in samples drawn in air. In thin films drawn in ESC agents, small blocks of the lamellae remain undrawn and attached to the fibrils drawn across micronecks. The ESC agents are suggested to weaken the cohesion between the fibrils in samples drawn beyond yield as well as the cohesion between mosaic blocks or similar structural elements in the original lamellae as they are being reoriented to form the fibrils. The stress is thus supported by a number of independent, nonuniform fibrils rather than a coherent structure; the weakest of these fibrils fail in turn as the crack propagates through the sample.

INTRODUCTION

Environmental stress cracking (ESC) is a condition of failure exhibited by polyethylene when subjected to polyaxial stresses while in contact with a nonsolvent, surface-active medium. If identical stresses are applied to the polymer in the absence of the stress crack-inducing medium, failure does not occur.

During the late 1950's and early 1960's, there was an intense amount of interest in the problem of ESC of polyethylene, largely because it was being widely used as an insulation and coating for telephone cable and underground pipework.[1] It was also used in flexble containers for soaps and detergents, which are active stress cracking agents.

The test most frequently used for ESC characterization in the United States is the bent strip test,[2] which is presumed to be representative of the stresses and strains encountered in use. In this test, ten polymer bars (1½ in. × ½ in. × ⅛ in.) are bent 180 degrees and immersed in a surface-active liquid (e.g., Igepal CO-530, General Aniline & Film Company, at 50°C). Each bar contains a longitudinal slit ¾ in. long × $^{2}/_{100}$ in. deep down the center of the upper face. Stress crack resistance is defined as the length of time required for five of the ten samples to show visible signs of cracking perpendicular to the slit. A photograph of several samples, in various stages of failure, is shown in Figure 1. As the samples subjected to the bent strip test progress toward failure, the original razor slit tends to deepen and widen, presumably as a result of strain-induced orientation. Following the opening of the slit, cracks (which are usually located near the base of the slit) begin to grow in a transverse direction. Figure 2 shows the

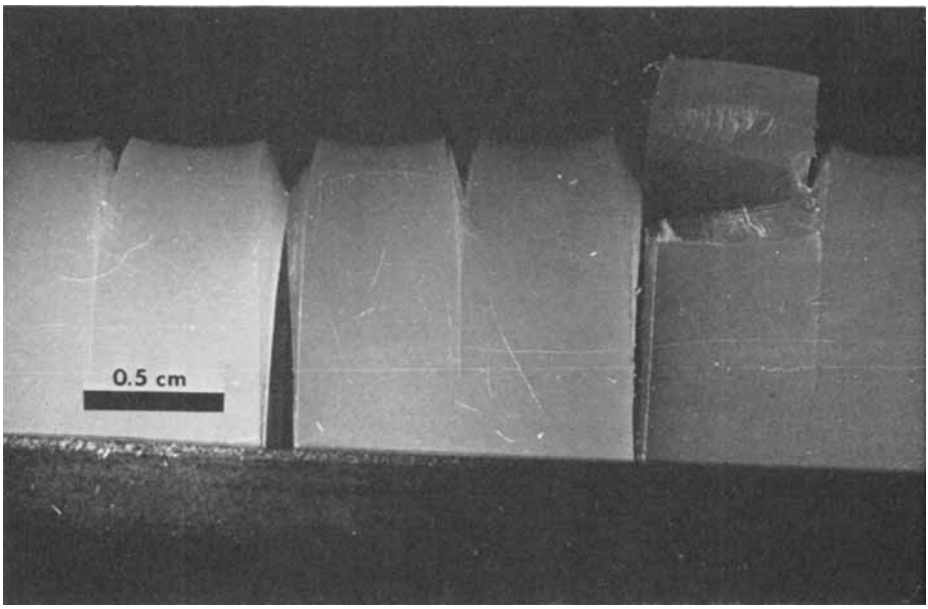

Fig. 1. Branched polyethylene samples at various stages of failure in the bent-strip test. The original razor slits have deepened and widened. Transverse cracks have started to form in the samples at left and center. Complete failure has occurred in the sample on the right.

inside of a test specimen just prior to failure. This specimen was sliced parallel to the original razor slit. The dotted line indicates the outline of the original razor slit. Following initiation, the transverse cracks grow slowly until they break through to the surface of the sample. Note that crack initiation occurs in the region where the polymer is stressed approximately to its yield point and not in the region of maximum stress.

The failure surface of the regions originally in tension appears quite smooth, whereas that of regions originally under compression seems extremely rough (Fig. 1). Most probably, total failure occurred very rapidly after the region in tension "cracked," yielding this result. However, when the smooth failure surface, which was originally under tension, is viewed by optical microscopy, it has a drawn, fibrous appearance (Fig. 3). This fibrous appearance we found to be common to all environmentally stress-cracked polyethylenes examined, to varying degrees, regardless of resin or cracking agent involved. This evidence indicates that ESC failure is not brittle.

In recent years, although practical means of improving the ESC resistance (such as molecular weight control) have been developed, little scientific interest has been reported in the process. Detailed knowledge of the mechanism should not only lead to improved materials, but should also contribute to an understanding of the general mechanism of tensile deformation of crystalline polymers. In particular, the origin of the fibrous texture of the deformed matter is of concern. In this paper we discuss the effect of the presence of an ESC agent on the tensile properties of notched and unnotched polyethylene bars and on the morphology of the resulting failure surfaces. In addition, the effect of the presence of an ESC agent on the ultrastructural deformation characteristics of thin films and single crystals is described. Commercial grades of polyethylene

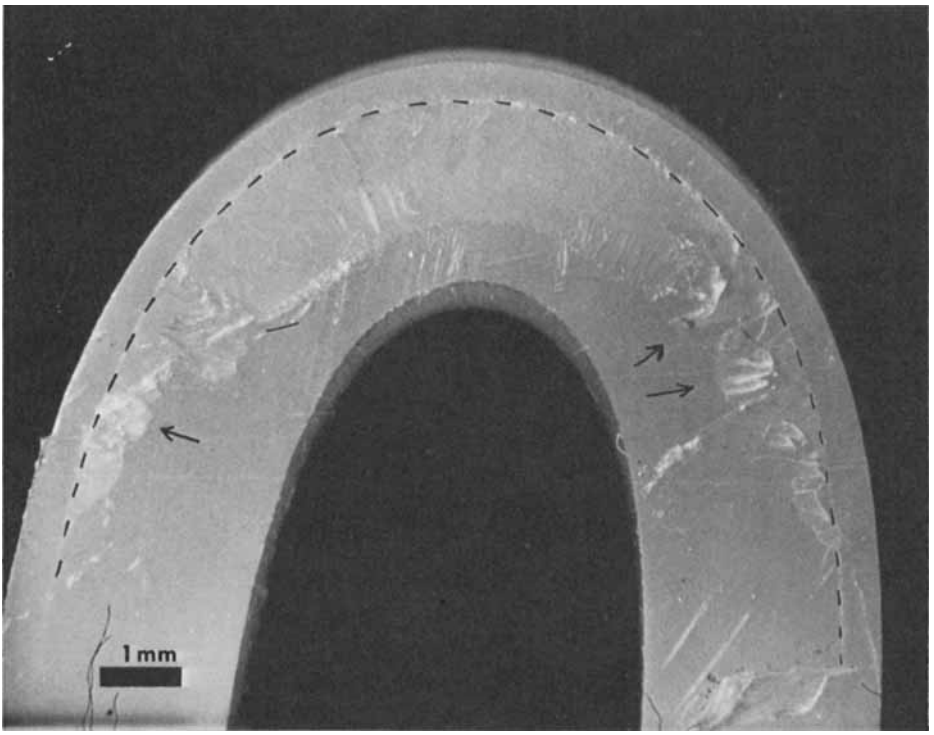

Fig. 2. Partially stress-cracked sample. The sample was cut along the razor slit after the slit had deepened and transverse cracks had just started to form. Cracks are appearing in the region marked with arrows.

with varying molecular weights and densities were used. The results of this study suggest that there is considerable potential for the techniques utilized, not only for understanding the mechanism of ESC, but also the mechanism of tensile deformation in general.

EXPERIMENTAL

Resins

The resins used for most of this research were Marlex (trademark of Phillips Petroleum Company for its polyethylene resins) 6002, 6015, 6050, 5040, and 5065 and Alathon (trademark of E. I. du Pont de Nemours and Company, Inc., for its polyethylene resins) 3B, 2020, and 4275. Marlex 6002, 6015, and 6050 are high-density (0.960 g/cc) resins having melt indices of 0.2, 1.5, and 5.0, respectively, as described by the sales literature for each resin. The ESC resistance determined by ASTM D1693-59T (bent strip test) is 60, 10, and 1 degrees F_{50}hr, respectively. Marlex 5040 and 5065 are intermediate-density (0.950) ethylene–butene copolymer resins with melt indices of 4.0 and 6.5. The ESC resistance is 20 and 10 degrees F_{50}hr, respectively. Alathon 3B, 2020, and 4275 are low-density (0.92 g/cc), free radical-polymerized polyethylene resins. The melt indices are 0.25, 1.1, and 3.7, respectively. The ESC resistance of Alathon 3B

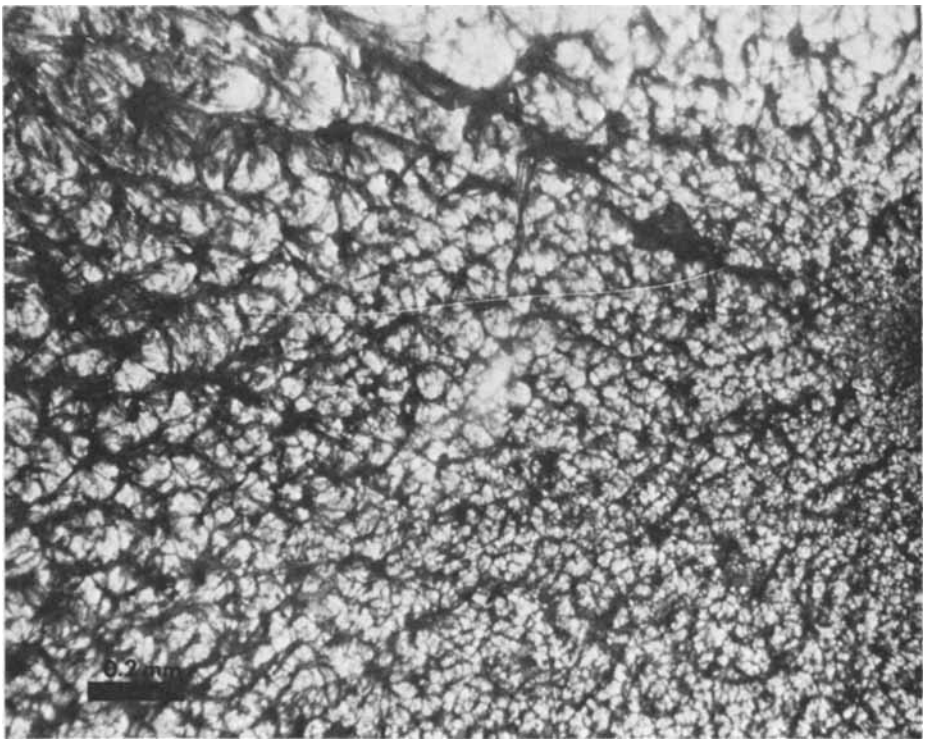

Fig. 3. Failure surface of a low-density polyethylene sample with good stress crack resistance from the bent-strip test. Scale represents 0.01 in.

is given as greater than 500 hr in the sales literature. Although not listed, the ESC resistance of Alathon 2020 is also very long, whereas that of Alathon 4275 is quite short. Some of the initial research was done using Alathon 3, 20, and 10. The corresponding values for the resins used were M.I. = 0.24, 2.2, and 2.0 and ESC resistance >1000 hr, 7 hr, and 10 min, respectively. As suggested by the ESC resistance and M.I., the two sets of resins cannot be directly compared.

Mechanical Properties

Tensile bars, 3 in. × ½ in. × ⅛ in. were cut out of sheets of various polyethylene resins which had been compression molded at 150°C and 40,000 pounds force for 5 min and quenched in ice water. A 0.020-in.-deep razor slit was made across the middle of each bar transverse to the tensile direction. These slits acted as stress risers. Sample bars of each resin were immersed in either methanol, isopropanol, or Igepal and drawn at rates of 5 cm/min and 0.5 cm/min in an Instron tensile testing machine. The failure surfaces of these samples were then compared to those of samples of the same resins drawn in air and water under the same conditions. Stress–strain curves were also measured, at a 5 cm/min strain rate, on microtensile specimens (1 in. gauge length, 0.25 in. width, 0.016–0.020 in. thick) while immersed in various liquids.

Measurements of stress relaxation in flexure and tension were made at room

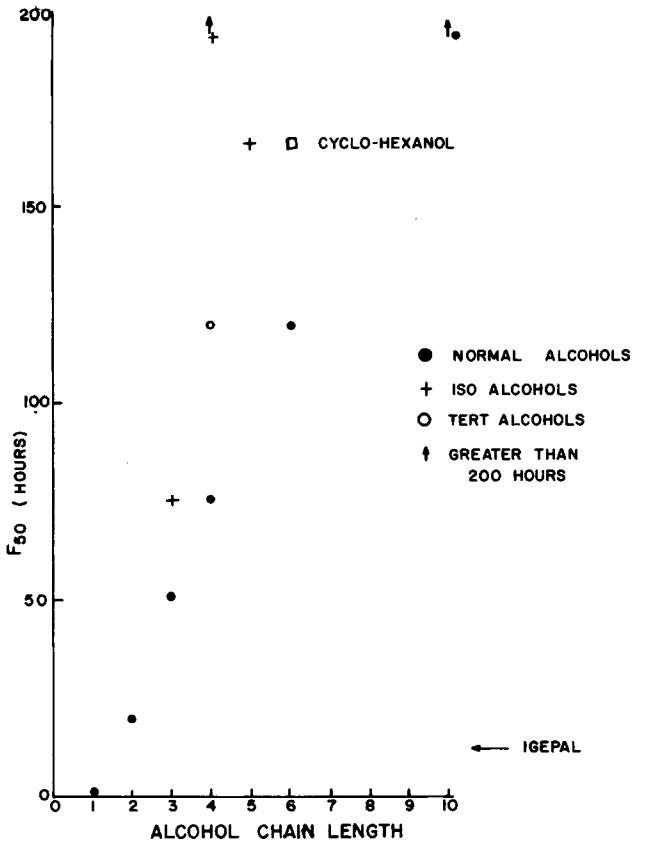

Fig. 4. Stress-crack resistance of samples of Alathon 20, as measured in the bent-strip test at room temperature, as a function of alcohol chain length. The ESC resistance in Igepal is also shown.

temperature in various cracking agents. For the flexure measurements, samples similar in size to those for the bent strip test for low-density polyethylene (1 in. gauge length, 0.125 in. thick, with and without a slit) were bent 0.2 in. at the center while immersed. The tension measurements were made on microtensile samples 0.009 in. thick, which were strained 0.05 in. and immersed in the liquid 1 min after the stress was applied.

Photographs, using a single-lens reflex camera, were made of the failure surfaces. These surfaces were also examined by scanning electron microscopy (SEM) and optical microscopy.

Thin Film Observations

Thin films were prepared from 1% solutions of various polyethylene resins in xylene. The solutions were cast hot onto strips of Mylar (trademark of E. I. du Pont de Nemours & Company for its polyester film) film fastened into stretch racks. After the xylene evaporated, the thin film specimens were remelted at 135°C or 150°C (depending on the resin used), recrystallized, and cooled to room temperature. These specimens were then deformed in air or in stress cracking environments and replicated with platinum and carbon for observation by transmission electron microscopy (TEM).

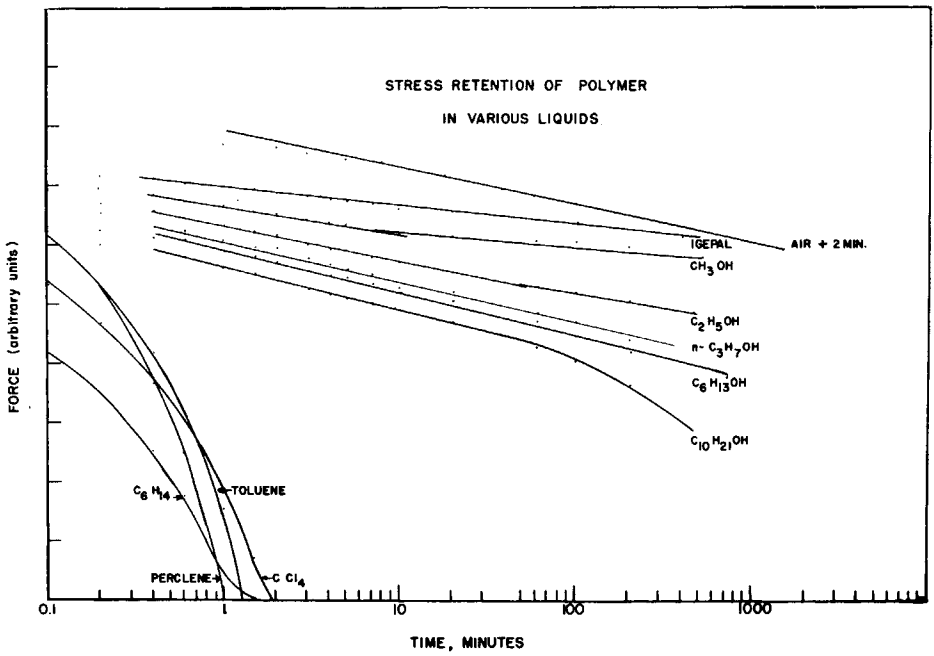

Fig. 5. Residual force of microtensile specimens strained 0.05 in. and immersed in the liquid listed 1 min after the stress was applied, plotted as a function of time of immersion.

Single Crystal Studies

Single crystals of the linear polyethylene resins (Marlex 6002, 6015, and 6050) were prepared by the self-seeding technique,[3] deposited on strips of Mylar film fastened into stretch racks, and subjected to deformation in various environments. The single crystals were shadowed with Pt–C after deformation. The resulting samples were examined by transmission electron microscopy.

Scanning Electron Microscopy (SEM)

The failure surfaces of the tensile bars were rotary coated with Au–Pd prior to insertion in a Cambridge S4-10 Stereoscan microscope. Micrographs were obtained in the secondary emission mode.

RESULTS AND DISCUSSION

Cracking Agent

Although one might expect such properties as surface tension or cohesive energy density of the ESC agent to affect the stress crack resistance in a readily interpretable manner, this does not seem to be the case. Figure 4 shows the bent strip test stress crack resistance of samples of Alathon 20 as a function of alcohol chain length; a regular progression is seen, the resistance increasing with chain length. For Alathon 3 and 10, however, a minimum in ESC resistance was found for chain lengths between 2 and 7. It is also noted that ESC failure in Igepal, which has a surface tension higher than that of any of the alcohols used, occurs just as rapidly as that in methyl and ethyl alcohol.

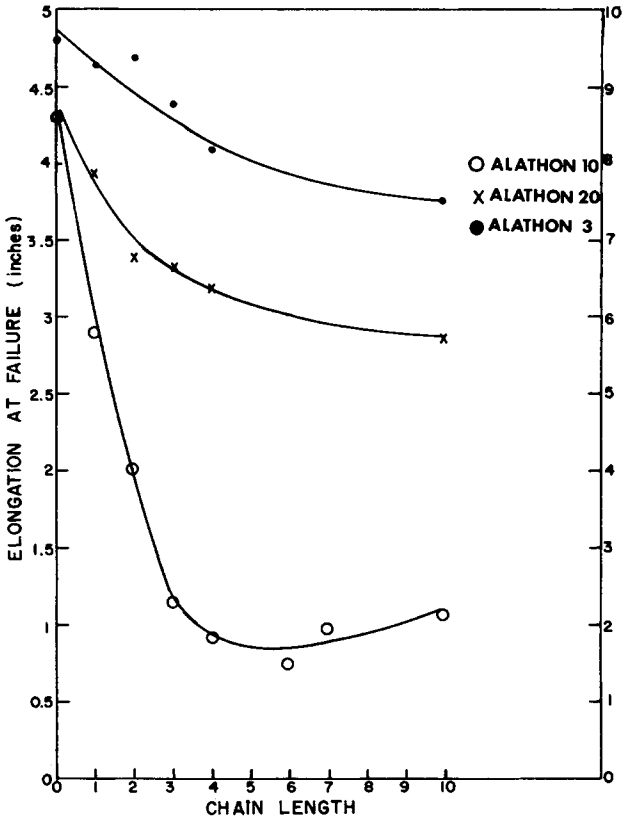

Fig. 6. Elongation at failure in various alcohols of three low-density polyethylene resins as a function of alcohol chain length.

Stress Relaxation

The stress relaxation measurements in flexure of the unslit bars of Alathon 10 were essentially the same whether in an air, water, or methyl alcohol environment. However, for slit samples (as in the bent strip test), the specimens, in the methyl alcohol environment cracked near the yield point. This observation is in agreement with the suggestion above that ESC failure occurs most readily in a polymer that is stressed close to its yield point.

Figure 5 shows a plot of residual stress versus time (measured from time of immersion) for samples immersed in various liquids. In general, it is seen that the rate of relaxation increased with increasing alcohol chain length. With decyl alcohol, curvature of the line indicates the start of solvation or swelling. In solvents such as toluene, the samples relaxed rapidly and then swelled. The linear nature of the data for some of the more active ESC agents indicate that they do not penetrate the sample and weaken it at these stresses; i.e., diffusion of the ESC agent into the stressed samples well ahead of any possible microcracks does not appear to be significant.

Tensile Tests

The elongation at failure of the microtensile specimens drawn at 5 cm/min in various alcohols is shown in Figure 6. In all cases it is seen that the elongation

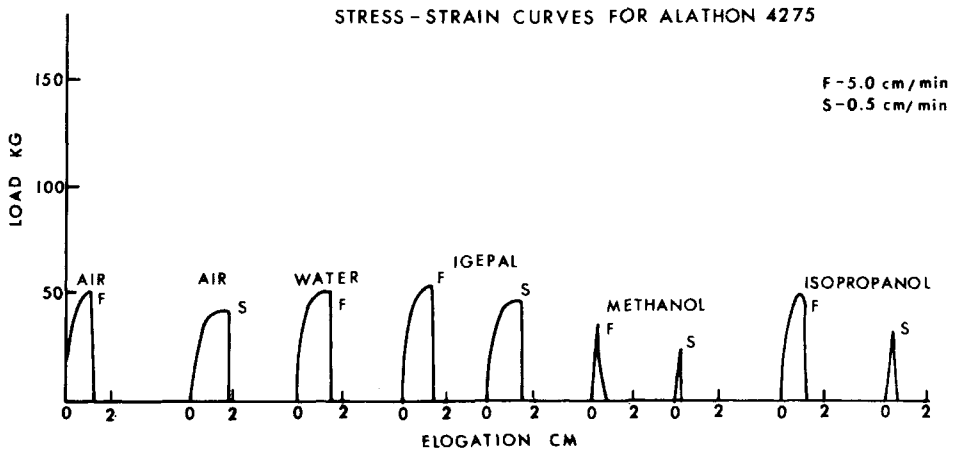

Fig. 7. Tensile force vs elongation curves for notched bars of Alathon 4275 drawn in various media.

decreases with increasing chain length; however, the failure occurs after yielding and neck formation even in the relatively low molecular weight samples of Alathon 10, which is the resin most susceptible to ESC.

Stress–strain curves for the notched samples of Alathon 4275 deformed in various media, at a strain rate of 0.5 and 5 cm/min, are shown in Figure 7. For identical strain rates, the curves are essentially the same whether the specimens were deformed in air, water (used to reduce any possible heating effect during

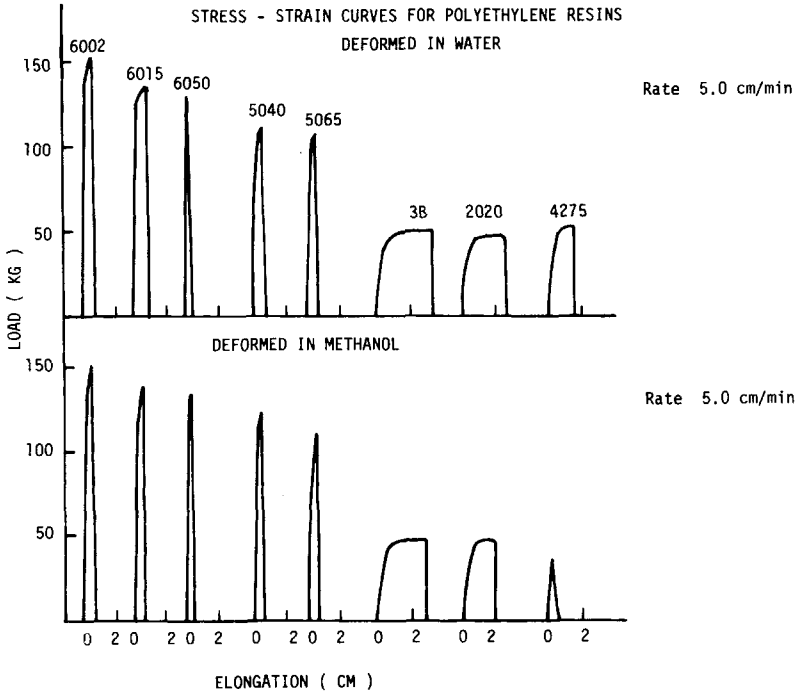

Fig. 8. Tensile force vs elongation curves for notched bars of various polyethylene resins drawn in water or methanol at 5 cm/min.

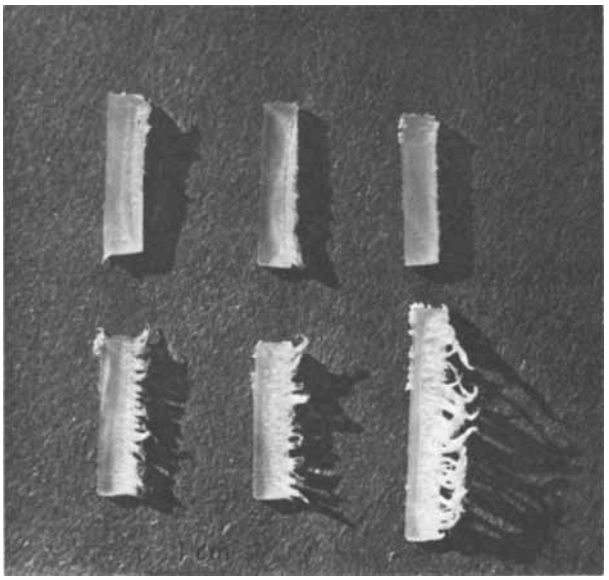

Fig. 9. Failure surfaces of Alathon 3B, 2020, and 4275 drawn in tension. The upper samples were drawn in air and the lower in isopropyl alcohol at a rate of 5 cm/min. The 0.020-in. razor slit is seen on the left-hand side of each specimen.

extension), or Igepal. Only in alcohol environment is an effect seen. Failure occurs more rapidly, with the samples failing more rapidly in methyl than in isopropyl alcohol. Note that this is opposite to the effect seen for the unnotched samples, in which the elongation at failure was less in isopropyl alcohol than in methyl alcohol. Also, failure occurs at somewhat lower elongations when the sample is drawn slowly in the alcohol than when it is drawn more rapidly.

For the other two low-density polyethylene samples, Alathon 3B and 2020, the curves for each sample, whether drawn in air, water, or any of the ESC agents used, are essentially the same and very similar to those of Alathon 4275 drawn in air, water, or Igepal, varying only with strain rate. In all of the notched samples, the total elongation was less than 3 cm. For the branched polyethylene resins, in general, higher elongations were attained for samples of higher molecular weight. As a result of the presence of the notch, deformation is localized to the vicinity of the notch. The measured elongation attained at failure corresponds to, or is less than, the extension of the resultant fibers (refer to Figs. 8 and 9) across the notch as observed after failure.

For the high- and intermediate-density polymers, the stress–strain curves for each samples were essentially the same, independent of the environment. Failure appears to have occurred at, or just prior to, the yield conditions. Typical curves for the various samples, drawn at 5 cm/min in water and methanol, are shown in Figure 8. Just as for Alathon 4275, notched tensile bars of all of the high-density samples failed at lower elongations, when drawn at the lower strain rate. Also, at this rate, the specimens exhibited considerable whitening, due to void formation, and nonrecoverable deformation. Stress–strain curves for the low-density polyethylene samples are also included for comparison purposes.

Despite the apparent similarity in most of the stress–strain curves for a given

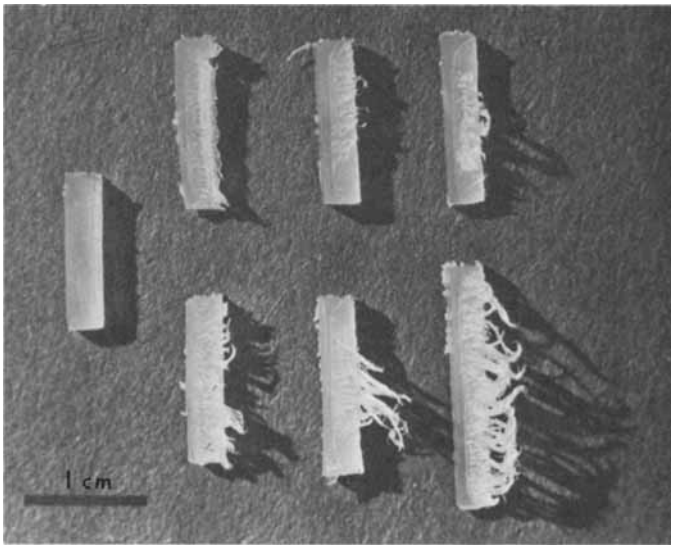

Fig. 10. Failure surfaces of notched bars of Alathon 4275 drawn in tension. From left to right, the samples were deformed in air, Igepal, methanol, and isopropyl alcohol. The samples on the top were drawn at a rate of 0.5 cm/min, whereas the air-drawn sample and those on the bottom were deformed at a rate of 5.0 cm/min.

resin, visual observation of the samples showed considerable differences in the failure process. The failure surfaces of the low-density resins drawn in air and isopropyl alcohol at 5.0 cm/min are shown in Figure 9. The failure surfaces of the samples drawn in air consist of a ridge of "collapsed" material, whereas those drawn in the ESC agent are highly fibrillar. Whether the samples were stressed in air or in isopropyl alcohol (or water or methyl alcohol), the total elongation, as measured on the stress–strain curve, was essentially the same for a given resin (except for Alathon 4275). This fact suggests that the ridge of material seen on the samples drawn in air (or water) has retracted. Contrary to the results of the stress–strain curves, which show an increase in elongation with molecular weight, the length of the fibers in the samples subjected to ESC conditions decreases with increasing molecular weight.

Figure 10 shows failure surfaces of samples of Alathon 4275 drawn in air, Igepal, methanol, and isopropyl alcohol, the samples being similar to those used for the stress–strain curves in Figure 7. As above, all samples drawn in the ESC agents have fibrous failure surfaces. The lengths of the fibers are considerably longer at the faster rate of draw. The sample drawn in air contains a ridge of "collapsed" drawn material. It is noted, in particular, that the longest fibers are observed on the failure surfaces of the samples which were drawn in methanol or isopropyl alcohol, even though the elongation at failure was smallest for these samples. The length of fibers observed, in fact, is approximately the same as the total measured elongation on the stress–strain curve, whereas the length of ridge of material on the air drawn sample is less than the measured strain value.

These observations suggest that an elastic recovery occurs in the material drawn in air, a recovery that does not occur, at least to the same extent, for the samples drawn in ESC agents. Two similar samples, drawn in isopropyl alcohol and observed from the surface opposite the slit, are shown in Figure 11. The splitting of the fibers is seen to extend all the way to the plane containing the slit,

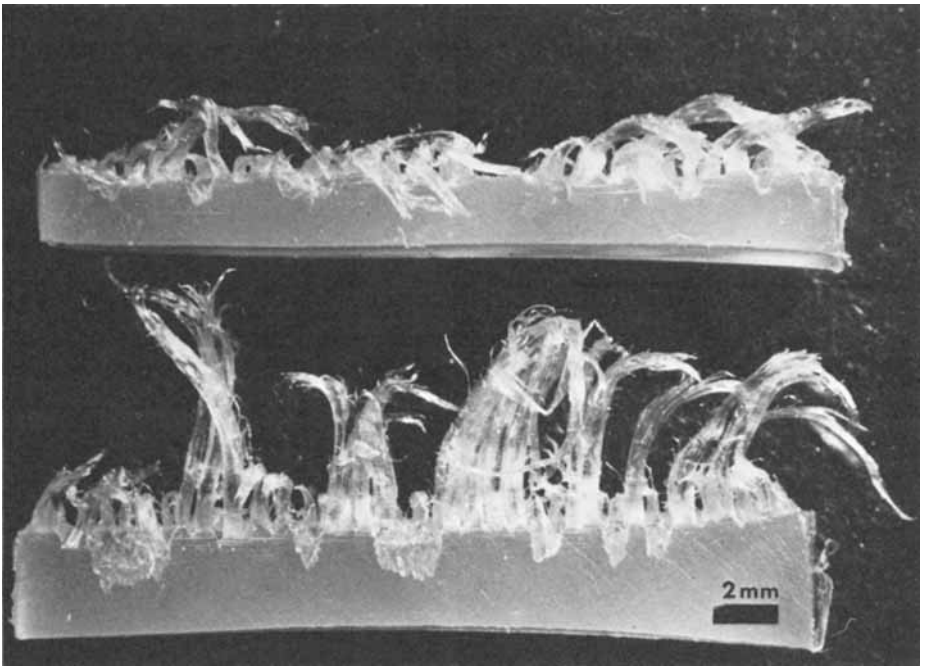

Fig. 11. Failure regions of an Alathon 10 sample drawn in isopropyl alcohol and photographed from the side opposite the slit.

with some material being drawn off the surface from a considerable distance beyond the slit plane in the regions in which the resulting long fibers are attached to the opposite failure surface.

On the basis of the above observations, the mechanism of deformation and the structure of the resulting fibrous material must differ between the samples drawn in ESC agents and for those drawn in air. In particular, it is evident that the cohesion of the fibers formed during elongation is considerably less for the samples drawn in the ESC agents. In conjunction with the observations of the site of ESC in the bent strip test, this suggests that one cause of ESC is this lack of cohesion; the small amount of transverse stress present is enough to cause the fibers to split apart. In the portions of the samples which have been stressed to yield, such that micronecking has occurred and fibers have formed, the fibers will act as independent entities in the presence of an ESC agent, whereas they will act as a more or less coherent structure in non-ESC environments. In the presence of ESC agents, the weakest and/or most highly stressed fibers fail. The load is then transferred to other fibers which fail in turn. That this is not the entire explanation, however, is shown by the observation that initial failure does not occur in the regions stressed beyond yield, regions in which a higher degree of fibrousness would be expected. The observations described below of thin films and single crystals drawn in ESC agents indicate that the mechanism of deformation, the process of forming the fibers, and the structure of the resultant fibers are also affected by the presence of the ESC agent.

Failure Surfaces

The failure surfaces of the bulk tensile samples were too rough to facilitate replication for TEM. However, SEM micrographs were obtainable and amply

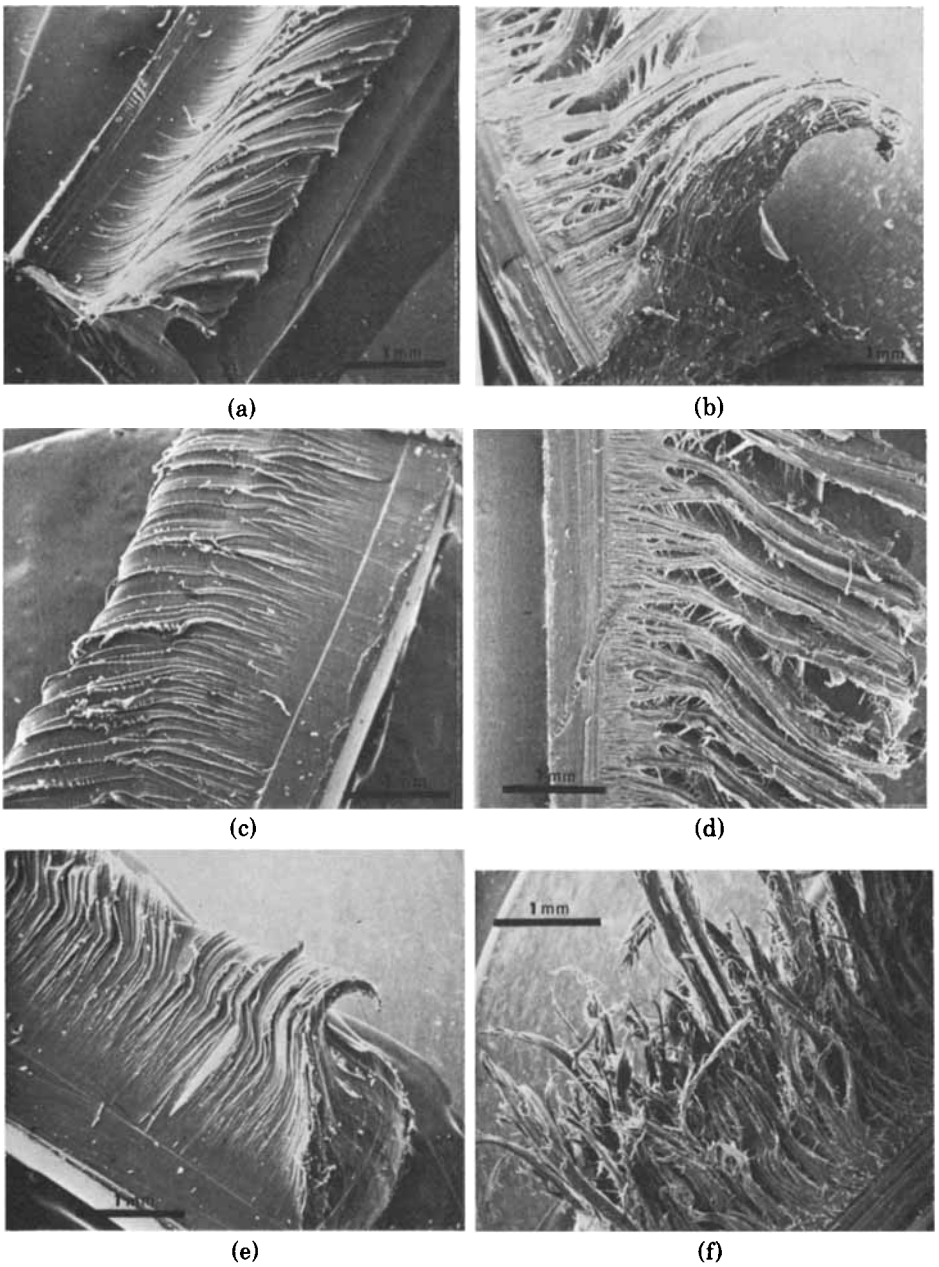

Fig. 12. Scanning electron micrographs of the failure surfaces of notched bars drawn at a rate of 5.0 cm/min. Alathon 3B drawn in (a) air and (b) isopropyl alcohol, Alathon 2020 drawn in (c) air and (d) isopropyl alcohol, and Alathon 4275 drawn in (e) air and (f) isopropyl alcohol.

confirmed the previous observations of a difference in character of the ESC and non-ESC deformed materials. Low-magnification SEM micrographs of the three low-density polyethylene resins, drawn at 5 cm/min in air and isopropyl alcohol, are shown in Figure 12. All surfaces are clearly fibrillar, but there is a significant difference in the cohesion of the fibrils. In the air-drawn samples, the ridge of collapsed material is seen to consist of a drawn fibrillar film that has curved back

(a) (b)

Fig. 13. Scanning electron micrographs of the failure surfaces of notched bars of Alathon 4275, deformed in (a) air and (b) isopropyl alcohol at a rate of 5.0 cm/min.

on itself. A smaller value of elongation at failure is attained for the sample of Alathon 4275 drawn in isopropyl alcohol than for that drawn in air (Fig. 6). However, the length of the drawn material is larger for the ESC agent-drawn samples, although the ratio does not appear as large as suggested in the photographs in Figures 9–11. Thus, the suggestions concerning a difference in mechanism of fiber formation would still seem to apply. The decrease in cohesion of the fibers is also seen at the fiber tips (see Fig. 13). The specimen drawn in air thinned down gradually, whereas that drawn in isopropyl alcohol tended to splay apart, with each individual fiber having a gradually thinning tip.

The fact that the air-drawn samples are fibrous, the fibers being more coherent, is shown in Figure 14. It is a higher-magnification picture of a portion of the drawn material in the samples of Alathon 4275 already shown in Figure 12. The

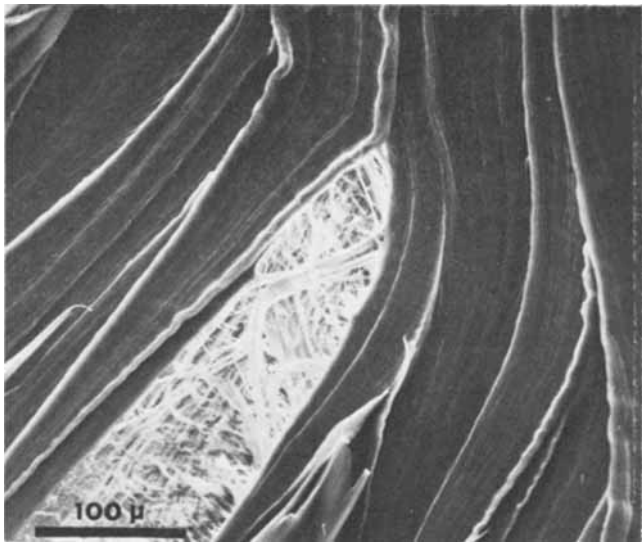

Fig. 14. Scanning electron micrograph of a fibrous region in the deformed material of the air-drawn Alathon 4275 sample.

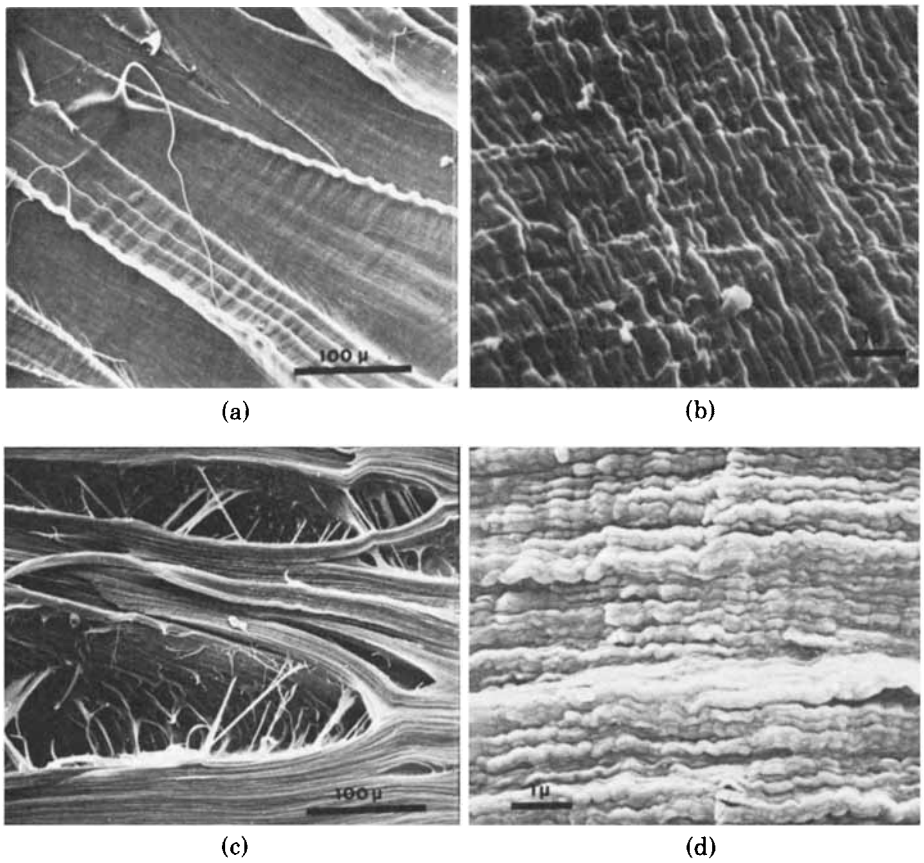

Fig. 15. Scanning electron micrographs of the failure material in a notched bar of (a, b) Alathon 2020 deformed in air and (c, d) Alathon 2020 deformed in isopropyl alcohol.

material split after shadowing but before or during insertion in the electron beam. Although it appears that the fibers along the edges of the cracks were originally present, it is not clear if they were originally present as basic structural elements or if they were formed by essentially a statistically random splitting of the drawn material.

In Figure 15 are shown several higher-magnification micrographs of the sample of Alathon 2020 deformed in air and isopropyl alcohol; 15(b) and 15(d) are higher magnifications of regions in 15(a) and 15(c). At these higher magnifications, both types of drawn material are seen to be corrugated. The corrugations run perpendicular to the draw direction. These corrugations presumably are a result of the retraction or recovery of the fibers after they were drawn out. The mechanism for such corrugating is unknown. However, it seems to indicate that the central portion of each fiber shrinks more than the outer portion. The degree of corrugation appears larger on the sample drawn in isopropyl alcohol. Despite the fact that the remaining fibers are longer in the samples drawn in isopropyl alcohol, this feature is also seen in the other two low-density resins.

The failure surfaces of the high-density samples all appear relatively smooth visually. By SEM, however, a fibrous texture, to varying degrees, is seen on all of the surfaces. Low-magnification micrographs of various surfaces (including

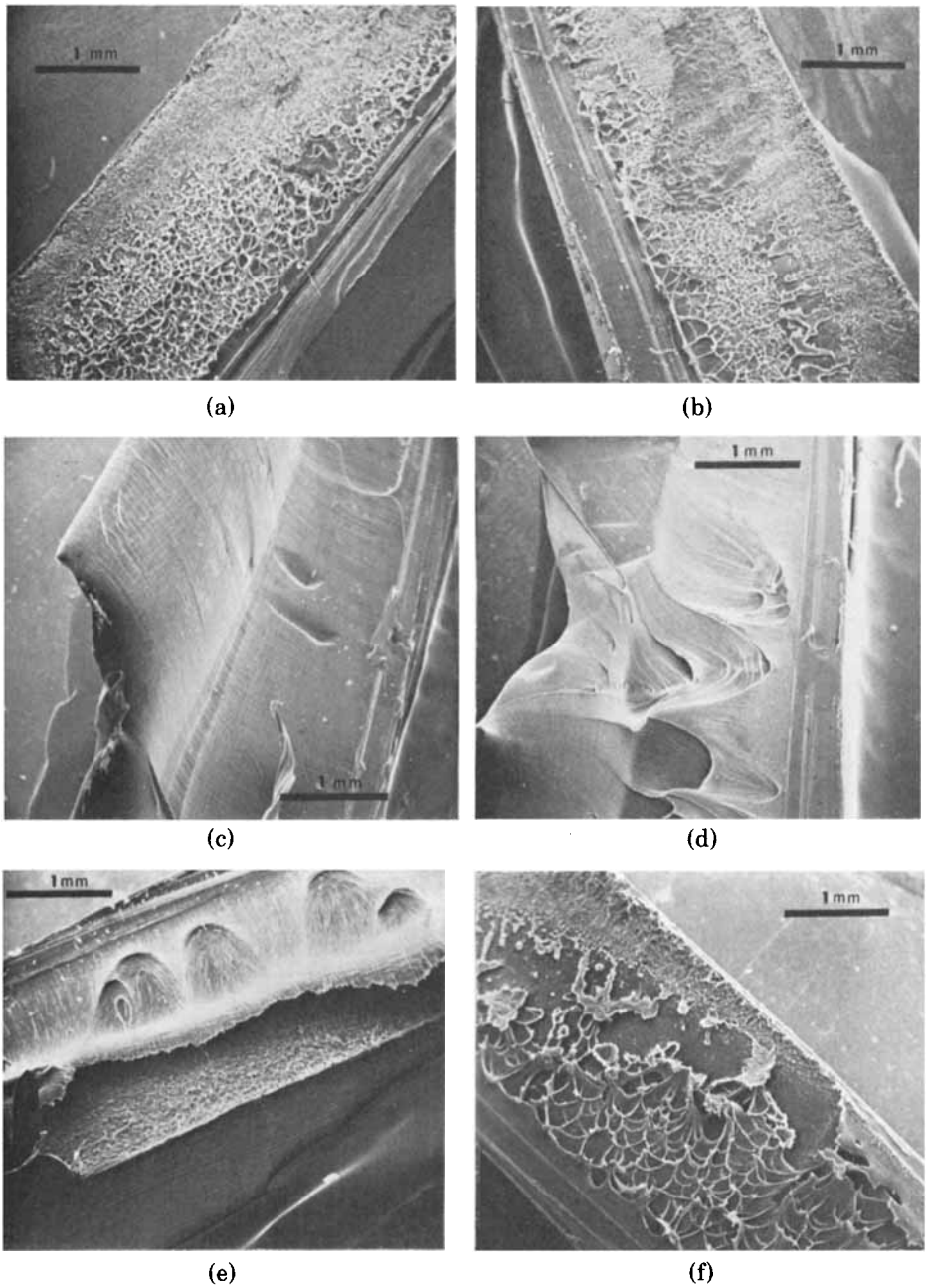

Fig. 16. Scanning electron micrographs of the failure surfaces of (a, b) Marlex 6050 deformed in air and isopropyl alcohol and (c, d) Marlex 6002 deformed in air and isopropyl alcohol, (e) Marlex 6015, and (f) Marlex 5040 deformed in isopropyl alcohol.

one micrograph of an intermediate-density Marlex 5040 sample) are shown in Figure 16. The failure surfaces for each of the resins shown in Figure 16, whether drawn in air or isopropyl alcohol, appear nearly identical even at higher magnifications. Only for the highest molecular weight material (Marlex 6002) is there possibly somewhat less cohesion, as indicated by a more fibrous texture, in the

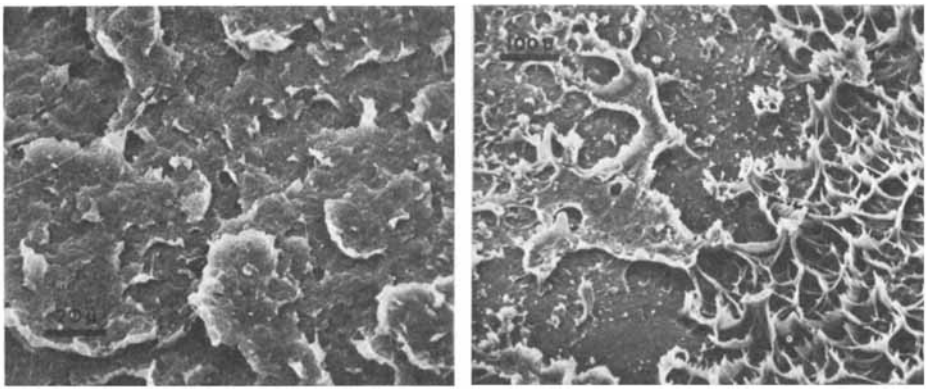

(a) (b)

Fig. 17. Scanning electron micrographs of the failure material of Marlex 6050 deformed in (a) air and (b) isopropyl alcohol.

sample drawn in isopropyl alcohol than in that drawn in air. Relaxation corrugations are seen in both Marlex 6002 samples.

In the low molecular weight (Marlex 6050) linear samples, both surfaces show a fibrous texture but on a much smaller scale. In addition, in both of these samples there is a band parallel to the surface opposite the razor slit in which a more brittle-type fracture has occurred. Figure 17 shows micrographs of these areas, with Figure 17(b) showing the transition to the fibrous surface also. It is believed that an interlamellar-type fracture has occurred. TEM replicas of these surfaces presumably would be similar to those obtained by fracture at liquid nitrogen temperatures, showing evidence of local deformation in which fibrils are formed and melt back to form mounds on the fracture surface.[4]

The micrographs of the intermediate molecular weight (Marlex 6015) sample drawn in isopropyl alcohol show some of both features [see Fig. 16(e)]. About half of the fracture surface consists of coherent drawn fibrillar material, while the other half is relatively smooth. At higher magnification, as shown in Figure 18, local deformation is seen to have occurred even in the relatively smooth area. However, on this surface also, in contrast to fibers observed on liquid nitrogen fracture surfaces, the fibers have remained extended.

Fracture surfaces of the intermediate-density resins also contain similar regions. In comparison with the higher-density samples, the "smooth" areas that are seen in the sample drawn in isopropyl alcohol are much smoother (see Fig. 19). The smoothness of these regions, interspersed among regions showing local deformation, may be due to a much smaller spherulite size inherent to these samples than in the higher-density samples. A somewhat rougher region in the samples drawn both in isopropyl alcohol and air, similar to that seen in the Marlex 6015 sample, is seen along the failure surface on the side opposite the razor slit [see Fig. 16(e)].

In summary, in agreement with the stress–strain curves, there appears relatively little difference between the failure surfaces of the high-density samples drawn in air and in isopropyl alcohol; it is certainly much less dramatic than the effects seen for the low-density resin samples. Practically, it is also known that linear polymers are less susceptible than branched polymers to ESC, although one of the advantages of the Marlex 5040 samples (with its low branch content)

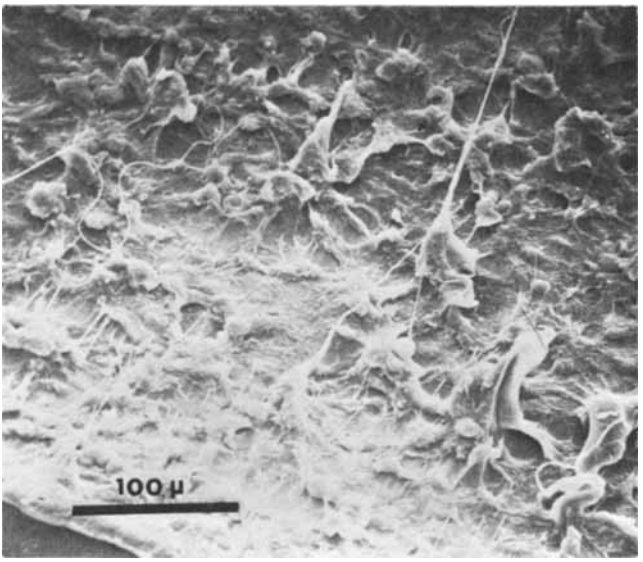

Fig. 18. Scanning electron micrograph of the failure surface of a notched bar of Marlex 6015 drawn in isoopyl alcohol.

is that it has better ESC resistance than the more linear samples. Another difference between the high- and low-density samples is their molecular weight distribution. This is known to affect ESC resistance. A narrow molecular weight distribution material has better ESC resistance than a broad molecular weight distribution polymer of the same average molecular weight.[5]

Thin Films

In as much as the primary difference in deformation behavior under ESC and non-ESC conditions was seen for the low-density samples, the deformation

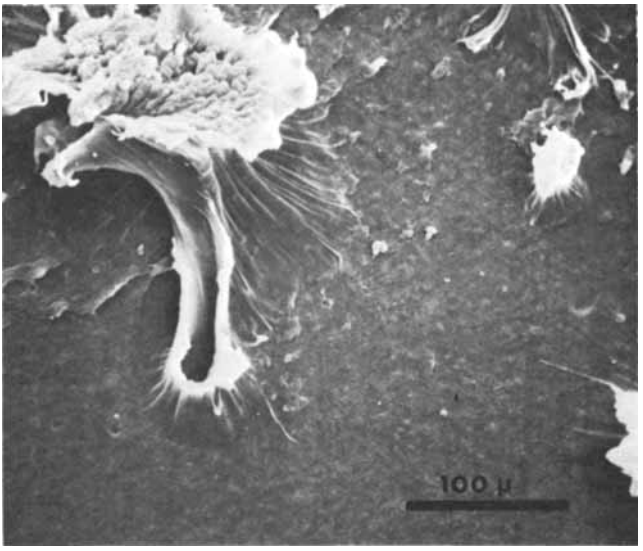

Fig. 19. Scanning electron micrograph of the failure surface of a notched bar of Marlex 5040 deformed in isopropyl alcohol.

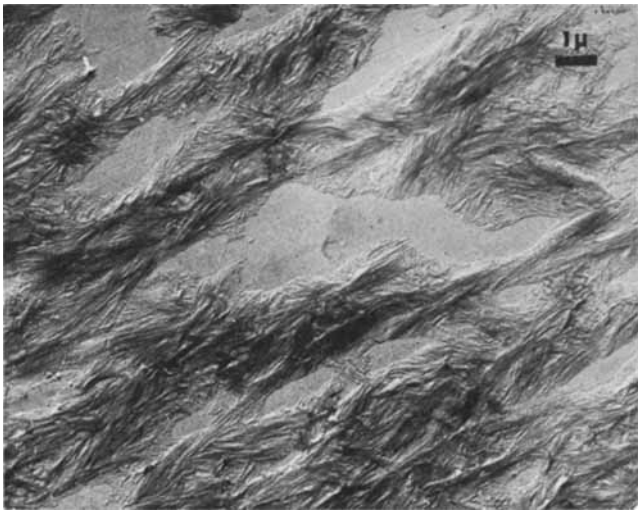

Fig. 20. Transmission electron micrograph of a thin film of melt-crystallized Alathon 4275 deformed 100% in air on a Mylar strip.

characteristics of thin films of Alathon 4275 were examined. Figure 20 shows such a film drawn 100% in air on a Mylar film. Only uniform, plastic deformation has occurred. The lamellae, in agreement with early work of Peck and Kaye,[6] seem to have twisted more or less as units into the draw direction. Presumably twinning, phase change, lamellar slip, etc., have occurred. No fibrils were seen in any of these samples, indicating that even incipient micronecking has not yet occurred although these samples have been drawn well beyond the yield elongation.

In order to characterize the structure of the fibrils in this resin, it was necessary to draw the thin films across cracks in a carbon substrate. By this method, high local deformations can be obtained. The resulting fibrils (Fig. 21) are smooth (similar to those observed previously for thick samples, thin films, and single crystals of linear polyethylene and other polymers drawn in air), with interfibrillar links of somewhat smaller diameters connecting adjacent fibers.

Figure 22 shows two micrographs representative of the results of drawing the thin films of Alathon 4275 (67% deformation) in methanol. Although plastic deformation similar to that observed in air still occurred, numerous regions were also observed in which micronecking has occurred.

It is noted that the fibrils formed remain coherent. This possibly is an artifact of the deformation process. The substrate shrinks laterally as it is being stretched, therefore compressing rather than separating the fibrils. The unique feature of these fibrils, however, is their roughness, as noted both by the bumpy surface and the uneven shadows. It is suggested that this roughness is due to mosaic blocks, as described by Peterlin,[7] or larger crystalline units having been torn off the edge of the crystalline lamellae and yet not having been completely incorporated into a fibril structure. On the larger pieces of material drawn along the fibrils, well-defined edges of the original lamellae can be seen. That is, not only is the cohesion of the fibrils themselves reduced by the presence of an ESC agent, but the deformation mechanism itself is changed. Possibly, the ESC agent also weakens the cohesion between the mosaic blocks in Peterlin's model. These

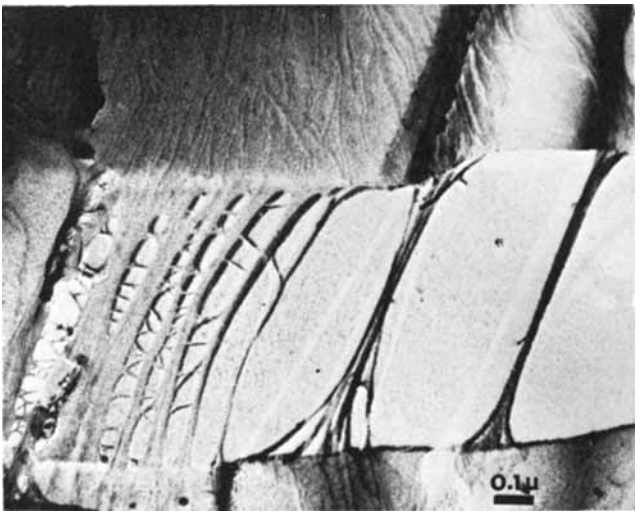

Fig. 21. Transmission electron micrograph of a thin film of melt-crystallized Alathon 4275 deposited on a carbon substrate on a Mylar strip. The Mylar was drawn 30%.

blocks then act as individual elements, many of which are only carried along as the fiber is formed rather than acting cooperatively. The tendency for elastic recovery of the fibers is reduced, as seen in the thick samples. According to Peterlin's model,[7] recovery during annealing is due to extended tie molecules connecting nonadjacent mosaic blocks.

Single Crystals

Although no essential difference was observed in the deformation characteristics of the thick, notched samples of the high-density polyethylenes, in the presence and absence of ESC agents, apparent differences were observed for single crystals of Marlex 6002 drawn on Mylar (see Fig. 23). (Single crystals grown from the low-density polyethylene are too small to permit significant observations.) As shown previously[8], linear polyethylene single crystals can be drawn on Mylar up to 100% elongation with only plastic deformation occurring. Cracks spanned by ca. 100-Å-diameter fibrils are seen occasionally. Usually, though, the presence of these cracks is restricted to regions of multiple superimposed lamellae. When drawn on carbon-coated Mylar film, smooth fibrils, often with interfibrillar links, are observed spanning the cracks.

In contrast, when the Marlex 6002 crystals were drawn on Mylar film while immersed in methanol (as shown in Fig. 23) or isopropyl alcohol, numerous cracks spanned by fibrils were observed. The fibrils, however, are smooth, showing no signs of the roughness observed in the fibers of low-density resins subjected to ESC conditions. We suggest that this tendency for the formation of numerous micronecks in the crystals drawn in ESC agents is again a result of weakened cohesion of the structural elements, presumably mosaic blocks, within the crystals. It is also possible, however, that the cracks resulted from weakened cohesion between the crystal and the substrate of Mylar films. An intermediate number of cracks were observed in crystals deformed while immersed in water, the cracks being present predominantly at the edges of the crystals.

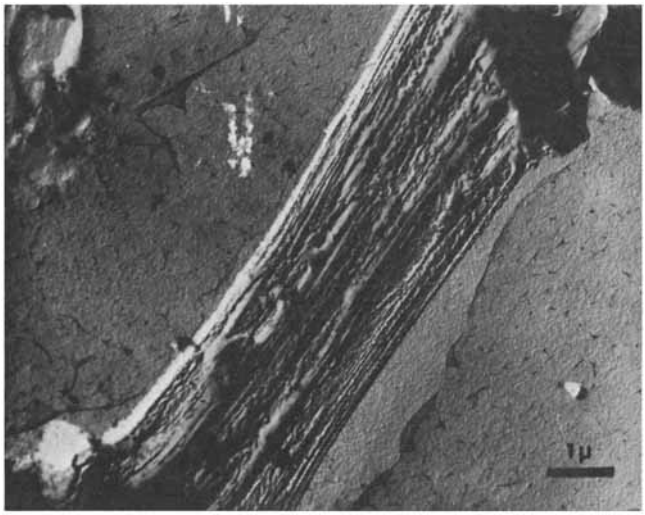

(a)

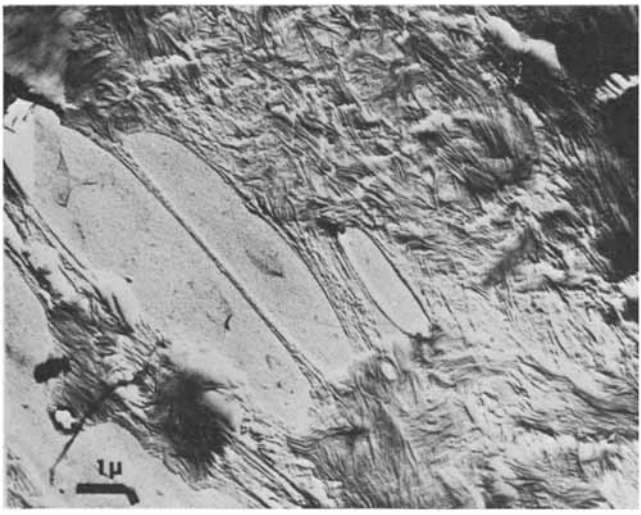

(b)

Fig. 22. Two transmission electron micrographs of a thin film of melt-crystallized Alathon 4275 deformed in methanol on a Mylar strip. The Mylar was drawn 67%.

CONCLUSIONS

It is obvious from the various micrographs that ESC of polyethylene does not result in brittle fracture, but rather is ductile in nature. Cracks are initiated in the regions where the material is strained near its yield point. Presumably, imperfections serve as stress risers and aid in the process. In particular, they introduce triaxial stresses that have a tendency to separate the fibers as they are formed. The normal drawing process in air involves a reorientation of lamellar structure (i.e., lamellar shear) and intralamellar deformation (molecular slip, tilt, twinning, etc.). In the presence of an ESC agent, the breakdown of the lamellae into mosaic blocks or larger units occurs more readily. These structures are reorganized as rigid entities in the fibers. Fewer extended tie molecules exist

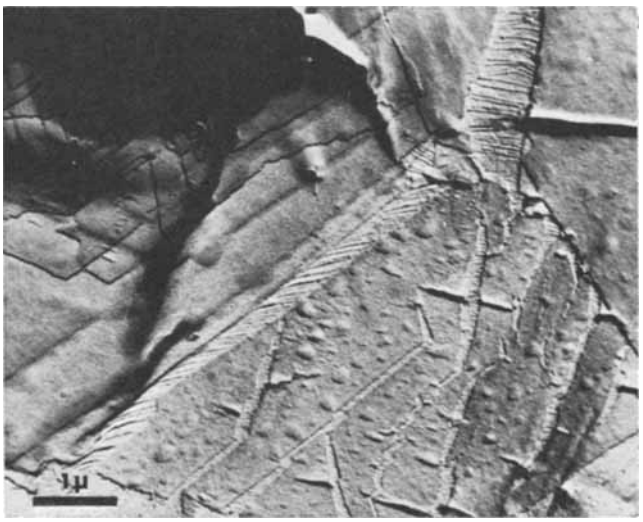

Fig. 23. Transmission electron micrograph of a single crystal of Marlex 6002 deformed 75% in the presence of methanol on a Mylar strip.

between nonadjacent mosaic blocks or crystallites, resulting in less recovery of the fibers when the tension is released by failure. It is suggested that the ESC agents, all of which are low surface-tension liquids, weaken both the cohesion between the fibers as well as the cohesion between the mosaic blocks or similar structural elements in the lamellae as they are reorienting for incorporation into fibers. On the macroscopic scale, the stress, in the bent strip test, for instance, is supported by a number of independent, nonuniform strands of drawn material. As the most highly stressed fibers break, the remaining fibers become more highly stressed and, in turn, fail. A crack propagates through the sample unless the stress is relieved. This occurrence also seems to be the case for the fibrils formed in single crystals and thin films.

The effect of the cracking agent in the stress–strain curve was seen to differ with and without a stress riser being present, the elongation at failure for the lowest molecular weight Alathon increasing with deformation speed and increasing alcohol chain length for the notched samples, while the opposite effect is seen for the effect of alcohol chain length for the unnotched samples (only one strain rate was used). This is presumably due to the difference in strain pattern in the sample; the razor slit is sufficiently deep that the region in its vicinity is drawn to failure without having the deformation progress into neighboring portions of the sample. We suggest that in the notched sample, as in the bent strip test and the thin films, the cracking agent affects both the mechanism of deformation and the cohesion between the drawn fibrils, whereas in the uniformly drawn thick samples, it primarily affects the cohesion between the fibrils after they are drawn. At this time, no conclusions can be drawn concerning the effect of type of cracking agent; the effect of surface tension or cohesive energy density was found to vary with the different resins.

Appreciation is expressed to the du Pont Company for permission to publish some results obtained while one of the authors (P.H.G.) was employed by them and to Phillips and du Pont for furnishing some of the resins used. The National Science Foundation is gratefully acknowledged for financial support of the recent research.

References

1. G. P. Marshall, N. H. Jenkins, L. E. Culver, and J. G. Williams, *SPE J.*, **28**, 26 (September 1972).
2. *Annual Book of ASTM Standards*, Designation: D1693-70.
3. D. J. Blundell, A. Keller, and A. Kovacs, *J. Polym. Sci.*, **B4**, 481 (1966).
4. P. H. Geil, *Polymer Single Crystals*, Wiley–Interscience, New York, 1963, Chap. 4.
5. J. B. Howard, *Engineering Design for Plastics*, E. Baer, Ed., Reinhold, New York, 1964, Chap. 11.
6. V. Peck and W. Kaye, *J. Appl. Phys.*, **25**, 1465 (1954).
7. A. Peterlin, *J. Mater. Sci.*, **6**, 490 (1971).
8. P. H. Geil, *Polymer Single Crystals*, op. cit., Chap. 4.

Received October 23, 1975
Revised July 23, 1976